ANTIMICROBIAL AGENTS AND CHEMOTHERAPY, Sept. 1996, p. 2160–2166 Vol. 40, No. 9
0066-4804/96/$04.00+0

Chemical Determinants of Antimalarial Activity of Reversed Siderophores

A. TSAFACK,[1] J. LIBMAN,[2] A. SHANZER,[2] AND Z. I. CABANTCHIK[1]*

Department of Biological Chemistry, Institute of Life Sciences, Hebrew University, Jerusalem, Israel 91904,[1] *and Department of Organic Chemistry, Weizmann Institute of Science, Rehovot, Israel 71600*[2]

Received 2 April 1996/Returned for modification 23 May 1996/Accepted 20 June 1996

Reversed siderophores (RSFs) are artificial hydroxamate-based iron chelators designed after the natural siderophore ferrichrome. The modular molecular design of RSF derivatives allowed the synthesis of various congeners with controlled iron-binding capacities and partition coefficients. These two physicochemical properties were assessed by a novel fluorescent method and were found to be the major determinants of RSF permeation across erythrocyte membranes and scavenging of compartmentalized iron. The partition coefficient apparently conferred upon RSFs two major features: (i) the ability to rapidly access iron pools of in vitro-grown *Plasmodium falciparum* at all developmental stages and to mobilize intracellular iron and transfer it to the medium and (ii) the ability to suppress parasite growth at all developmental stages. These features of RSFs were assessed by quantitative determination of the structure-activity relationships of the biological activities and partition coefficients spanning a wide range of values. The most effective RSF containing the aromatic group of phenylalanine (RSFm2phe) showed 50% inhibitory concentration of 0.60 ± 0.03 nmol/ml in a 48-h test and a 2-h onset of inhibition of ring development at 5 nmol/ml. The lipophilic compound RSFm2phe and the lipophilic and esterase-cleavable compound RSFm2pee inhibited parasite growth at all developmental stages whether inhibition was assessed in a continuous mode or after discontinuing drug administration. The antimalarial effects of RSFm2phe and cleavable RSFm2pee were potentiated in the presence of desferrioxamine (DFO) at concentrations at which DFO alone had no effect on parasite growth. These studies provide experimental evidence indicating that the effective and persistent antimalarial actions of RSFs are associated with drug access to infected cells and scavenging of iron from intracellular parasites. Moreover, the optimal antimalarial actions of RSFs are apparently also determined by improved accessibility to critical iron pools or by specific interactions with critical parasite targets.

Like all living organisms, malaria parasites depend on iron for growth and replication. This property makes them susceptible to iron deprivation, which can be induced by treatment with iron chelators (4, 5), as shown in in vitro cultures of *Plasmodium falciparum* (17, 23, 26), in animal models of malaria (11, 18, 22), and in human trials (3, 14, 30) with the clinically approved agent desferrioxamine (DFO). However, despite its advantages, DFO lacks the requisite speed of action and therapeutic efficacy to serve as a reliable substitute or additive for the treatment of severe cases of malaria, in particular, multidrug-resistant strains (33). Most other synthetic or naturally occurring chelators showed significant weaknesses as well, because they were apparently not free of undesirable side effects (15, 25).

Despite a plethora of studies on iron chelation and malaria, it is still unclear which factors are responsible for the high degree of susceptibility of protozoan parasites to chelator-induced iron deprivation relative to the susceptibility of mammalian organisms. Recently, we applied a series of synthetic chelators of variable lipophilic-hydrophilic balance (28) whose antimalarial actions were assessed as a function of parasite stage dependence, time of drug exposure and dosage, and reversibility of action. New information gained from this application allowed us to propose a working model for iron chelator action on parasites (4, 5, 20). In that model, the primary stage of iron utilization was the trophozoite stage, in which the metal was mobilized from degraded hemoglobin (5), as recently proposed (1, 12). The iron chelators which were retained within the parasites showed the most persistent inhibitory effects whether they were applied before, during, or after the stage of major iron utilization (5, 20, 31). An advantage of the model was its ability to predict the antimalarial potencies of combinations (5, 13) of chelators with different permeation properties, which could generate a synergistic mechanism of action (31).

An equal degree of uncertainty exists regarding the factors which contribute to the antimalarial performance of iron chelators (4, 5). The single empirical factor which has been assessed systematically in terms of its contribution to antimalarial efficacy was the drug partition coefficient (PC) (4, 19, 25). Moreover, structure-activity relationships (SARs) were only established for a group of reversed siderophores (RSFs) (19, 28), while permeation into cells was only studied with a selected group of fluorescent iron chelators (4) and with ^{59}Fe complexes of RSFs and DFOs (19).

In the present work we expanded the gamut of RSFs with agents of higher lipophilicities and hydrophilicities, including hydrophobic RSFs with enzymatically cleavable ester groups that can generate hydrophilic-impermeant RSFs intracellularly. Our studies indicate that whereas all RSFs were effective iron scavengers in solution, their PCs determined their ability to penetrate into cells, scavenge iron, and exert an antimalarial effect. This was apparent in the SAR schemes. SARs were assessed over a wide range of drug lipophilicities, as given by the PC and model membrane permeation constant. The marked antimalarial effect of RSFm2phe, the most lipophilic RSF tested, led us to propose that its therapeutic efficacy might involve either a unique mechanism of drug accessibility to

* Corresponding author. Phone: 972-2-6585420. Fax: 972-2-6586974. Electronic mail address: ioav@cc.huji.ac.il.

critical iron-containing components of the parasite or a specific interaction with them.

MATERIALS AND METHODS

Materials. The chemical structures of the RSFs used in the study are depicted in Fig. 1. The agents were synthesized and chemically analyzed by modifications of previously published methods (8). They comprise the basic compound RSFm2 and the analogs RSFm2pee and RSFm2pa, whereby pee denotes the propionic acid ethyl ester and pa denotes the propionic acid moieties extending from the hydroxamate groups of the binding cavity. RSFm2phe carried a two-carbon (m2) spacer linking the amino acid phenylalanine to the tripodal anchor. RSFm2(H) denotes the demethylated analog of RSFm2. DFO was obtained from Ciba-Geigy (Basel, Switzerland). All other chemicals were from Sigma Co. (St. Louis, Mo.) or were the best available grade. [^{3}H]hypoxanthine was from the Radiochemical Centre (Amersham, Little Chalfont, United Kingdom). All solutions were prepared in deionized, charcoal-filtered water.

Synthesis of chelators. (i) Preparation of Tris hydroxamate RSFm2(H). The protected Tris hydroxamate was prepared by dissolving 6.0 g of the parent triacid (9) in 25 ml of dry acetonitrile to which a solution of 7.0 g of *O*-benzylhydroxylamine in 10 ml of acetonitrile was added; this was followed by the addition of 300 mg of hydroxybenzotriazole and 3.6 ml of diisopropyl carbodiimide under ice cooling. The resulting mixture was allowed to warm to room temperature and was left for 2 days under stirring. The resulting crude reaction mixture was concentrated to dryness and was purified by chromatography on silica gel (the eluent was $CHCl_3$-iPrOH, where iPr is isopropanol; yield, 2.6 g of protected Tris hydroxamate).

A sample of 200 mg of protected Tris hydroxamate dissolved in 30 ml of ethanol was treated with 80 mg of Pd/C (1/10) and was hydrogenated under atmospheric pressure at room temperature for 3.5 h. Filtration of the mixture and concentration of the filtrate provided 104 mg of Tris hydroxamate RSFm2(H).

Preparation of Tris ester RSFm2pee. The parent tris acyl halide was prepared from 6.0 g of the parent triacid (9), which was dissolved in 30 ml of dry, ethanol-free chloroform (dried by passing through basic alumina) and which was treated dropwise with 12 ml of oxalyl chloride and 60 drops of dimethyl formamide, whereupon gas evolution was observed. The reaction mixture was stirred overnight at room temperature and was subsequently concentrated in vacuo to dryness under conditions of exclusion of moisture. The crude material was characterized by its infrared absorption at 1,792 cm^{-1} (in dry chloroform). Half of the crude triacyl halide was dissolved in 15 ml of dry and ethanol-free chloroform and was treated dropwise (under ice cooling) with a solution of 7.5 g of $HNOBnCH_2CH_2COOEt$ (where Bn is benzyl and Et is ethyl) (34) in 20 ml of chloroform and with 5.8 ml of Et_3N. The reaction mixture was allowed to warm up to room temperature and was left under stirring overnight. Completion of the reaction was determined by infrared analysis (disappearance of the acyl halide peak at ca. 1,792 cm^{-1}). The crude product was concentrated in vacuo; suspended in 300 ml of ethyl acetate; washed twice with water, twice with 1 N aqueous HCl, twice with water, twice with 1 N aqueous $NaHCO_3$, and again twice with water; dried with $MgSO_4$; filtered; and concentrated. Chromatography on silica gel (with chloroform with increasing amounts of ethyl acetate as the eluent) provided 3.18 g of pure protected Tris ester product.

The Tris ester of RSFm2pee was prepared by dissolving 720 mg of the protected Tris ester in 50 ml of ethanol and treating it with H_2 (atmospheric pressure) and 280 mg of Pd/C (10%) at room temperature. The suspension was filtered, and the filtrate was concentrated to provide 460 mg of RSFm2pee.

The protected Tris acid of RSFm2pa was prepared by dissolving a sample of 100 mg of the protected Tris ester in 20 ml of methanol and treating the mixture with 2 ml of 1 N aqueous NaOH for 1 h and subsequently with additional portions of 2 ml of 1 N aqueous NaOH until all material had been hydrolyzed ($CHCl_3$-MeOH [where Me is methyl], 9-1; thin-layer chromatography). Then, the solution was acidified, concentrated, treated again with base (1 N $NaHCO_3$) to pH 8, washed with ethyl acetate, acidified, and extracted with ethyl acetate. Washing with water and drying with $MgSO_4$ provided the protected Tris acid.

The Tris acid RSFm2pa was prepared by dissolving 1.19 g of protected Tris acid in 60 ml of absolute ethanol and reacting it with H_2 under atmospheric pressure for 1.5 h in the presence of 350 mg of Pd/C (10%). The resulting mixture was filtered and concentrated to provide 825 mg of Tris acid RSFm2pa (~99% purity).

Preparation of RSF-Phe. Pentachlorophenolate $CbzNHCHBnCOOC_6Cl_5$ was prepared by dissolving 8.0 g of Cbz-phenylalanine in 150 ml of acetonitrile and treating the mixture with 7.2 g of pentachlorophenol and 320 mg of dimethylaminopyridine and cooling the mixture to ice temperature (4°C) and reacting it with 4.2 ml of diisopropyl carbodiimide overnight at room temperature. The mixture was concentrated and filtered through neutral alumina (containing 5% water) to provide 10.36 g of active ester.

The hydroxamate CbzNHCHBnCONOHMe was prepared by dissolving 4 g of phenolate dissolved in 20 ml of dry methylene chloride and treating the mixture overnight with a suspension of 630 mg of *N*-methylhydroxylamine hydrochloride, 1.1 ml of triethylamine, and 85 mg of *N*-hydroxysuccinimide in 15 ml of methylene chloride. Purification by chromatography over silica provided the pure hydroxamate.

The hydroxamate $H_2NCHBnCONOHMe$ was prepared by dissolving 1.25 g of hydroxamate in 80 ml of absolute ethanol and hydrogenation for 3 h under atmospheric pressure at room temperature in the presence of 550 mg of 5% Pd/C. Filtration and concentration provided 550 mg of amino hydroxamate.

The Tris hydroxamate RSFm2phe was obtained by reacting 1.7 g of the parent Tris carboxylate active ester (9) dissolved in 40 ml of dry methylene chloride with a solution of 1.65 g of amino hydroxamate, 200 mg of N-hydroxysuccinimide, and 100 mg of imidazole in 30 ml of methylene chloride at room temperature. The overnight reaction yielded a mixture which was concentrated and chromatographed through silica (with $CHCl_3$-MeOH as the eluent) to provide the pure (~99%) Tris hydroxamate.

Chemical properties of chelators. The chelator structures were determined by infrared, UV-visible, circular dichroism, and nuclear magnetic resonance imaging methods as described elsewhere (8, 34).

(i) PCs. Estimation of the PCs of the various RSFs was based on determinations of the RSFs' distributions in octanol:water (saline) after overnight incubation as described previously (28).

(ii) Iron-binding affinity of chelators in solution. The iron-binding affinity method was based on the application of the probe calcein (CA), whose fluorescence (488- and 517-nm excitation and emission maxima, respectively) is quenched by stoichiometric concentrations of iron upon binding (2). Fluorescence recovery obtained by the addition of a competing chelator and the rate and extent of recovery provide a measure of the RSFs' ability to scavenge iron from CA-iron complexes. The measurements were done in *N*-2-hydroxyethylpiperazine-*N*′-2-ethanesulfonic acid (HEPES)-buffered saline (HBS; pH 7.2; 20 μmol of HEPES per ml and 150 μmol of NaCl per ml). The fluorescence of 0.5 nmol of CA per ml was prequenched with 1 nmol of a freshly prepared solution of ferrous ammonium sulfate per ml. The rate of restoration of the fluorescence was followed by using a concentration of 5 nmol/ml for each chelator. Fluorescence was measured in either a PTI station (PhotoMed, Wede, Germany) or a Spex Fluorolog II Spectrometer (Spex Industries, Edison, N.J.).

(iii) Scavenging of iron from resealed erythrocyte ghosts. The CA incorporated into erythrocyte ghosts encapsulation, as described previously (6), was induced to lose virtually all its fluorescence by the addition of membrane-permeant iron(II) added as ferrous ammonium sulfate (FAS). Removal of residual extracellular iron and CA was done by washing the ghosts with a solution containing the nonpermeant chelator diethylenetriaminepentaacetic acid and gel filtration through a Sephadex G-50 coarse column (Pharmacia, Uppsala, Sweden). An aliquot of resealed ghosts (10^7/ml) was diluted in HBS, and fluorescence was recorded with time as described above. The rate of fluorescence recovery induced by a given chelator provided a measure of the permeation of the drug into the ghost, with maximal fluorescence recovery attained by the addition of the fast-permeating chelator salicylaldehyde isonicotinoyl hydrazone (SIH) (23 μg/ml). The pseudo-first-order rate constant of fluorescence recovery (k) was calculated by linear regression of the normalized traces on the basis of the equation $\ln([F_\infty - F_t]/[F_{\infty - F_0}]) = -kt$, where F_0, F_t, and F_∞ represent the fluorescence intensities at times zero, t, and infinity (after the addition of SIH), respectively.

Biological properties of RSFs. (i) Antimalarial activity. The cultivation method used was a modified version of that of Trager and Jensen (29), as described elsewhere (28). Parasitemia and growth stage distribution were determined on methanol-fixed and Giemsa-stained smears. The antimalarial activities of the free RSFs or their respective iron complexes were assayed as described previously (28, 31). Briefly, the compounds were added from concentrated stock solutions in dimethyl sulfoxide to microculture plates (24 wells; Costar, Cambridge, Mass.) containing infected erythrocytes (2.5% hematocrit and 2 to 5% parasitemia). Twenty-four hours after incubation with the indicated drug, the cells were supplemented directly with 6 μCi of [^{3}H]hypoxanthine per ml or the drugs were washed off three times with a large volume of RPMI 1640 medium and were replenished with fresh growth medium before the addition of radiolabel. All systems were run in sextuplicate. Parasite growth was assessed for a further 24 h by harvesting the frozen-thawed lysate of labeled cells onto glass fiber filters (Tamar Inc., Jerusalem, Israel) on which the macromolecules were deposited. The incorporation of label into the nucleic acids was measured on a Beckman scintillation counter. The 50% inhibitory concentrations (IC_{50}s) were determined by nonlinear least-square fit to sigmoidal functions (10). All data are given as average ± standard errors (SEs). Inhibitory actions resulting from the combined actions of two different drugs were assessed by the additive and independent concept of mode of action as described by Poch (21). The theoretical values for each of these two modes of action of drug combinations were statistically compared with the experimental ones by t tests by using the Jandel Scientific software Sigma Plot for Windows.

(ii) Mobilization of cell labile iron. *P. falciparum* cultures of 15 to 30% parasitemia were pooled, and the various parasitic stages were separated over a Percoll gradient as described elsewhere (24) by using alanine instead of sorbitol. The cells were washed and resuspended in RPMI 1640 without phenol red growth medium, supplemented as described above for normal cultures with HEPES, glucose, $NaHCO_3$ and heat-inactivated human plasma. The number of cells was determined by counting in an improved hemocytometer chamber (Neubauer). The iron mobilized from cells by iron chelators was determined at different time intervals after mixing the extracellular medium with an equal volume of acetone, followed by overnight incubation at −70°C, for

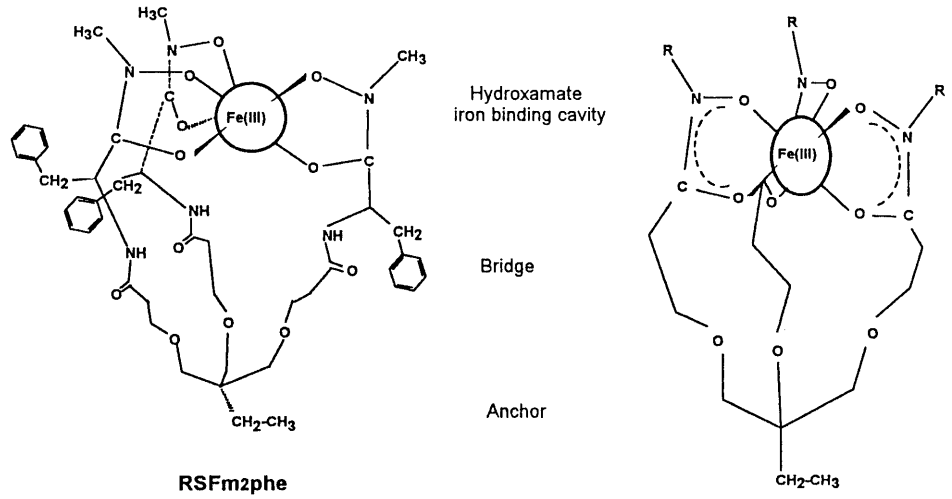

RSF	R
m_2	CH_3
$m_{2(H)}$	H
m_{2pa}	CH_2CH_2-COOH
m_{2pee}	CH_2-CH_2-$COOCH_2CH_3$

FIG. 1. Chemical structures of RSFs. RSFm2 and RSFm2(H) are the methylated and demethylated forms of members of the RSF tripodal family (8, 28) which form the hydroxamate iron-binding cavity. RSFm2pee and RSFm2pa are RSFm2 analogs possessing propionic acid ethyl ester and propionic acid residues, respectively, that extend from the hydroxamate iron-binding cavity. RSFm2phe is a structural congener which carries phenylalanine residues between the anchor and the hydroxamate-binding cavity.

deproteinization. The labile iron in infected and noninfected cells was assessed by cell lysis in the presence of a protease inhibitor cocktail (17 μg of phenylmethylsulfonyl fluoride per ml, 10 μg of benzamidine per ml, 3.7 μg of tosyl phenylalanyl chloromethyl ketone per ml, 3.7 μg of tosyl lysylchloromethyl ketone per ml, 10 μg of leupeptin per ml, and 1 μg of pepstatin per ml) and the indicated chelator. Cell lysis was done by three cycles of freezing in liquid nitrogen and thawing in a water bath. The lysate was cleared from the particulate material by centrifugation at 10,000 × *g* and 4°C and was deproteinized as described above. Estimation of the amount of labile or chelated iron was carried out by the ferrozine method (7) with fresh preparations of FAS as the standard. Ferrozine [3-(2-pyridyl)-5,6-bis(4-phenylsulfonic acid)-1,2,4-triazine] solution (247 μg/ml) was prepared in 9.2 μg of mercaptoacetic acid per ml–5.8 μg of thiourea per ml. The pH was adjusted to 5 in order to minimize the probable contamination by heme iron. An equal volume of this solution was added to the test samples for generation of the iron-ferrozine complex. The absorption was read against the ferrozine solution at 562 nm in a Milton Roy Spectronic 3000 Array spectrophotometer. Samples of cell-free medium were treated and used for subtraction of the background iron in the medium. Medium from cells which were not exposed to the respective chelators had essentially the same iron levels as cell-free medium. Data are given as averages ± SEs.

RESULTS

Figure 1 depicts the various derivates of RSFs that were used in the study. All RSFs used in the study have the tripodal form, possessing either substituents that extend from the hydroxamate-binding cavity or an aromatic amino acid (phenylalanine) as a bridge between the triscarboxylate and the hydroxamate-binding cavity. The compounds examined included RSFm2(H), which represents the demethylated form of RSFm2(CH_3) (referred to in this work as RSFm2) and the RSFm2pee and RSFm2pa analogs.

The chemical properties of the various RSFs, which are depicted in Table 1, comprised the octanol:water (saline) PCs and the iron-binding affinities of the chelators relative to that of DFO. Table 1 also depicts the permeability constants for the respective RSFs measured in erythrocyte membrane ghosts and the antimalarial activity (48 h of continuous exposure to drug, starting from ring stages), which is given in terms of the IC_{50} of the drug.

The quantitative SARs of the RSFs as antimalarial agents assessed in in vitro cultures are given in Fig. 2 in terms of inhibitory potency versus the agent's lipophilicity.

All the RSFs used in the present study had similar iron-binding affinities (Table 1), and their iron-bound complexes had no inhibitory effects on *P. falciparum* in culture (data not shown). Hence, the major determining factor in the antimalarial potency was apparently the agent's ability to access critical intracellular iron pools, as determined by the PC. The SARs held for all RSFs used in previous studies (19, 28) and in the present one, which included the most extreme examples of lipophilic and hydrophilic congeners.

An additional indicator of drug potency, which is dictated by the drug permeation properties, is the time required by a given drug concentration to exert an inhibitory effect on parasite

TABLE 1. Properties of RSFs

RSF	Octanol:water PC	Relative iron binding[a]	k (s^{-1} [10^{-4}])[b,c]	IC_{50} (nmol/ml)[c,d]
m2	1.7	0.65	1.80 ± 0.06	3.0 ± 1.0
m2(H)	0.11	0.44	1.10 ± 0.04	92 ± 18
m2pa	0.12	0.58	0.70 ± 0.05	275 ± 25
m2pee	13.5	0.76	3.2 ± 0.1	2.9 ± 0.3
m2phe	40	1	3.9 ± 0.8	0.6 ± 0.3

[a] Iron binding is expressed relative to a value of 1.16 for DFO (19).
[b] The permeation rate constant (k) is for entry into resealed erythrocyte membrane ghosts.
[c] Data are given as averages ± SE.
[d] IC_{50}s were determined at 48 h by nonlinear least-square fit to sigmoidal functions (10).

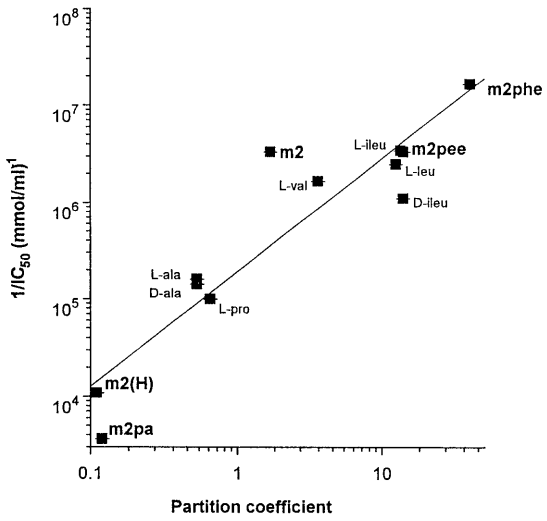

FIG. 2. Quantitative SAR of the in vitro antimalarial actions of RSFs (inhibitory potencies). The antimalarial actions of the RSFs, given in terms of the reciprocals of the IC_{50}s, were correlated with the respective PCs (data taken from Table 1). The line corresponds to the regression for an apparent linear fit ($R = 0.9$, $n = 12$, $P < 0.0001$). D and L refer to the respective amino acid isomer in the RSF structure (27).

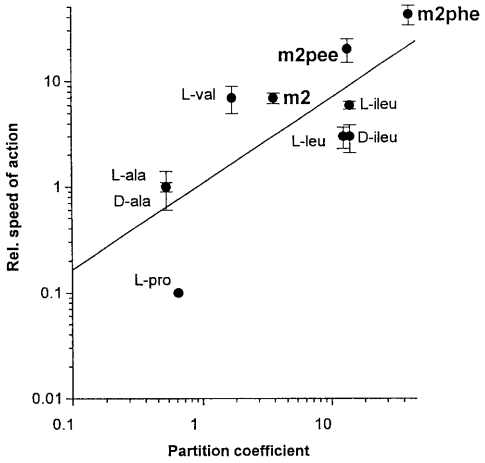

FIG. 4. Quantitative SAR of the in vitro antimalarial actions of the RSFs (speed of action). The correlation between the speed of action of the RSFs (given as percent inhibition of nucleic acid synthesis after 6 to 8 h of exposure relative to the IC_{50} measured at 48 h of exposure) and the PCs is presented. The line is the regression line for an apparent linear fit ($R = 0.77$, $n = 10$, $P < 0.01$). D and L refer to the respective amino acid isomer in the RSF structure (27).

development. As depicted in Fig. 3, the onset of inhibition of nucleic acid synthesis differed for the various chelators used at equal concentrations. In cultures composed of early rings, the most lipophilic agents affected parasites within 4 h of exposure. We have assessed the speed of action of the drug by following nucleic acid synthesis in the presence of various concentrations of chelators for 6 h. The normalized speed of action presented in Fig. 4 was determined as the percent inhibition attained at 6 h divided by the IC_{50} of the drug obtained in the 48-h test

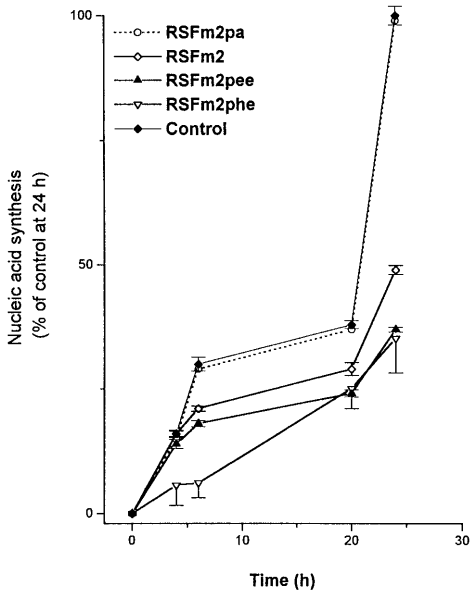

FIG. 3. Time course of inhibition of nucleic acid synthesis by selected RSFs. The time dependence of nucleic acid synthesis is given relative to that for the control at 24 h, as followed in synchronized cultures (starting at the ring stage) in the presence of the indicated RSFs (5 nmol/ml). The control and RSFm2pa gave essentially indistinguishable results. Datum points are depicted as means ± standard errors of the means.

(full cycle of growth). This normalized measure of speed of action was found to correlate with the PCs for all the agents which had detectable effects on parasite growth.

The relatively high degrees of potency of the lipophilic iron chelators at early stages of parasite development prompted us to assess also their modes of action on the parasites, following the working model presented elsewhere (4, 20). The first prediction is related to the production of persistent inhibitory effects at the stage of parasite development in which iron mobilization is limited, i.e., the ring stage (4). Parasites at the ring stage were exposed to various concentrations of RSFm2phe and RSFm2pee for 24 h, and nucleic acid synthesis was assessed in the continued presence of drug or after removal of the drug from the growth medium. The two experimental systems are denoted either continuous treatment or discontinuous treatment, respectively (Fig. 5). The data indicate that for either agent administered at the ring stage, most of the inhibitory effect was essentially irreversible. This was particularly the case for RSFm2pee, which although it was relatively less potent than RSFm2phe, it had the advantage of potentially serving in the cells as a precursor of the impermeant RSFm2pa. Thus, the putatively cell-generated RSFm2pa apparently induced persistent effects on parasite development because of its retention within the cell.

The second predictive feature of the model was the possibility that RSFs may potentiate the inhibitory action of the poorly permeant and slowly acting DFO (31). We analyzed the effects of RSFm2pee and RSFm2phe in combination with DFO at relatively ineffective concentrations (5 and 10 nmol/ml) on parasite growth using Poch's analytical method (21) for distinguishing between additive and independent modes of action of pairs of drugs (Fig. 6).

The data indicated that for either drug, the combined action of the drug in combination with DFO used at biologically ineffective concentrations was statistically more potent than the predicted additive or independent effects. Such higher than additive levels of action of RSFs and DFO reinforced the validity of the phenomenon which was observed with other RSF congeners (13, 31) and the suggested modes of action of the drugs (31).

The third predictive feature of the model is the commonly

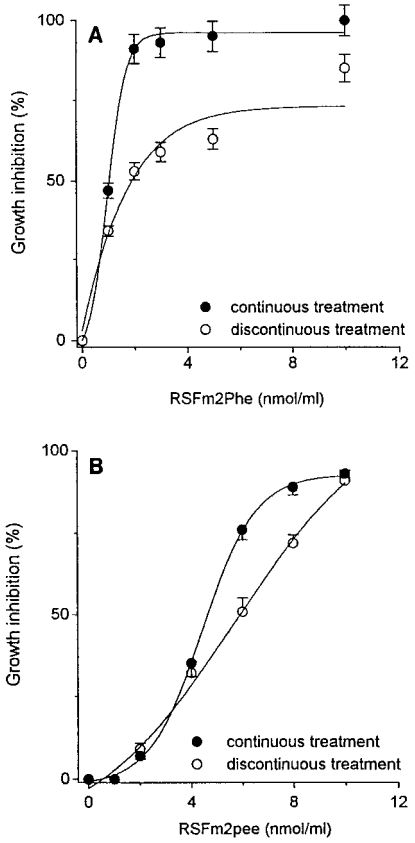

FIG. 5. Reversible and irreversible modes of action of RSFs. RSFm2phe (A) and RSFm2pee (B) were assessed on synchronized ring-stage parasites (in sextuplicate) treated with the indicated concentration of drug for 24 h. After washing with medium, half of the cultures were incubated with the same concentration of drug (continuous treatment) and half were incubated with medium alone (discontinuous treatment). Growth inhibition (mean ± standard error of the mean) is given in terms of nucleic acid synthesis relative to the value obtained for control cultures (no drug).

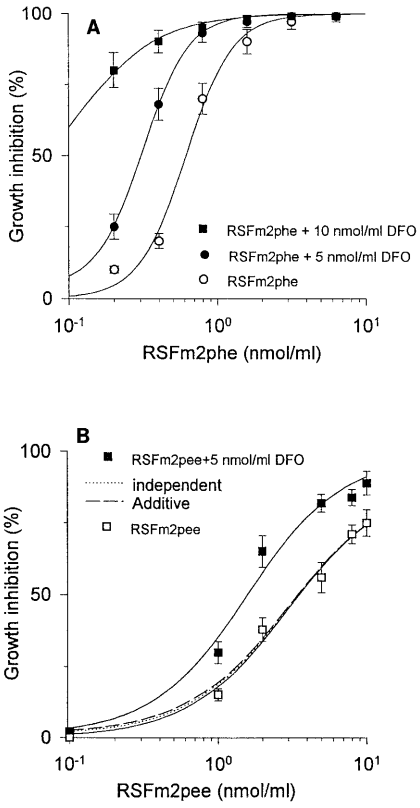

FIG. 6. Combined actions of RSFs and DFO. DFO was used in combination with various concentrations of either RSFm2phe or RSFm2pee on a full cycle of parasite growth (starting at the ring stage). The percentage of growth inhibition (mean ± standard error of the mean; $n = 6$) was plotted against the drug concentration. Full lines represent sigmoidal fits through experimental points. Poch's analyses (21) for either the additive or the independent actions of the drugs were considerably shifted to the right of the experimental lines (shown only for RSFm2pee). The respective IC_{50}s of RSFm2phe (A) were as follows: (i) experimental, 0.60 ± 0.03 nmol/ml (DFO = 0, nmol/ml), 0.31 ± 0.01 nmol/ml (DFO = 5 nmol/ml), and 0.07 ± 0.01 nmol/ml (DFO = 10 nmol/ml); (ii) theoretical-additive (Poch [21], 0.46 ± 0.07 nmol/ml (DFO = 5 nmol/ml) and 0.16 ± 0.01 nmol/ml (DFO = 10 nmol/ml); (iii) theoretical-independent (Poch [21]), 0.59 ± 0.02 nmol/ml (DFO = 5 nmol/ml) and 0.25 ± 0.04 nmol/ml (DFO = 10 nmol/ml). The theoretical values for the additive and independent models were significantly different from the experimental data ($P < 0.001$). The respective IC_{50}s of RSFm2pee (B) were as follows: (i) experimental, 2.9 ± 0.3 μg/ml (DFO = 0 nmol/ml) and 1.58 ± 0.25 μg/ml) (DFO = 5 nmol/ml); (ii) theoretical-additive (Poch [21]), 2.38 ± 0.05 μg/ml (DFO = 5 nmol/ml); (iii) theoretical-independent (Poch [21]), 2.60 ± 0.08 μg/ml (DFO = 5 nmol/ml). The theoretical values for the additive and independent models were significantly different from the experimental data ($P < 0.001$).

accepted, but hitherto not experimentally shown, correlation between the inhibitory potency of the drug and its capacity to extract iron from infected cells. This was carried out in the present study with various RSFs applied at the different stages of parasite development. Parasites were exposed for 2 to 4 h to either RSF and were analyzed for the iron that they extracted from the cell into the medium. Figures 7 and 8 depict data obtained for RSFm2phe alone, and Table 2 compiles the data obtained for the different drugs.

As shown in Figure 6, the amount of iron extracted into the medium increased with time of exposure to the drug and varied with the stage of parasite growth. The amount of iron extracted after 2 h of exposure to chelator was highest at the trophozoite stage and lowest at the schizont stage. This amount further increased over the subsequent 2 h (4 h total), particularly in trophozoites. Since, as shown before, RSFm2phe penetrates very fast across membranes and scavenges intracellular iron, the amount of iron extracted between 2 and 4 h provides a measure of the release of free iron within the parasite. Indeed, the total amount of chelatable or labile iron present in infected cells (Fig. 8), that is, the amount of iron which chelators can extract when added to lysed cells, was also highest for the trophozoites stage, but it was also significant for the ring stage. The high value of iron availability and scavenging found at the trophozoite stage is in line with both the high levels of hemoglobin degradation and the chemical release of iron induced by glutathione and other factors, characteristic of that stage of development (1, 12).

In Table 2 we present the values of iron mobilization by all the RSFs used in the study and assessed at all stages of parasite development. Impermeant agents such as RSFm2pa or RSFm2(H) were virtually ineffective in extracting iron at any stage of parasite growth. For all other agents, the data indicated that the mobilization of iron into the medium was highly dependent on the drug's lipophilicity (Table 1) and iron availability (labile iron) at the particular stage of parasite development (Fig. 7). The relatively higher level of extraction of iron from parasitized cells by RSFm2 compared with that by RSFm2pee, despite RSFm2pee's higher degree of lipophilicity, could be attributed, in part, to some intracellular formation of impermeant RSFm2pa from RSFm2pee or to differences in

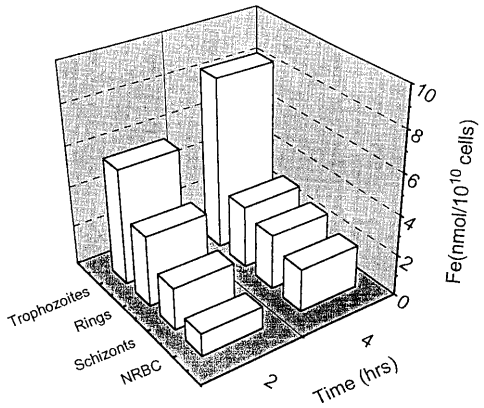

FIG. 7. RSF-mediated extraction of iron from parasitized cells. Iron mobilization into the medium by RSFm2phe at 2 and 4 h of exposure of different developmental stages of *P. falciparum* is presented. The iron-chelator complex mobilized into the medium was monitored by the ferrozine method as described in Materials and Methods. NRBC, normal erythrocytes.

molecular size. Yet, the antimalarial efficacies of these two agents were not significantly different.

DISCUSSION

The present study constitutes a new effort in our pursuit of antimalarial agents with improved biological performance. It focuses on a family of hydroxamate-based agents whose molecular structures could be modulated in order to confer on the molecules defined chemical properties (28). The RSFs were previously shown to curb malaria parasite growth in vitro in a manner commensurate with their PCs (20, 28). This chemical property was shown to contribute to the speed of action, the efficacy, and the stage specificity of the drug (20, 31). A previous SAR study with RSFs showed a positive correlation between IC_{50} and PC, although the repertoire of RSFs spanned a limited range of PC values (19, 28). The most hydrophobic RSFs markedly outperformed the classical hydroxamate DFO (5, 31) in all the biological parameters mentioned above. However, despite their relative faster action profiles and wider stage specificities, RSFs were less effective than DFO in producing persistent effects, particularly at the most metabolically active and drug-sensitive stage of parasite growth, the trophozoite stage (19). In recent studies we have combined the unique properties of hydrophobic RSFs and DFO and obtained major improvements in their antimalarial actions (13, 31).

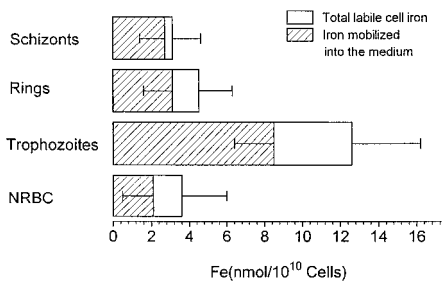

FIG. 8. Total labile cell iron and its RSF-mediated extraction from parasitized cells. The amount of iron mobilized into the medium (hatched portion) after 4 h of exposure of the cells to RSFphe is indicated. Data are given as values relative to that for the total labile cell iron. NRBC, normal erythrocytes.

TABLE 2. Iron mobilization by RSFs in normal and infected cells

RSF	Iron mobilization[a]			
	NRBC[b]	Rings	Trophozoites	Schizonts
m2	0.8 ± 0.3	2.2 ± 0.7	3.1 ± 1.2	3.0 ± 1.0
m2(H)	0	1.2 ± 0.4	2.1 ± 0.5	1.0 ± 0.3
m2pa	0	0	<0.1	0
m2pee	0.5 ± 0.2	2.6 ± 0.8	3.4 ± 1.9	0.7 ± 0.2
m2phe	1.7 ± 0.5	3.7 ± 1.8	8.5 ± 2.6	3.0 ± 0.7

[a] Data are mean ± standard error of the mean of at least three separate experiments, given as nanomoles of Fe per 10^{10} cells, mobilized into the growth medium after 4 h incubation of the cells with 20 nmol of the indicated chelators per ml. Statistical comparison by the Student t test showed that the amount of iron mobilized from trophozoites was significantly ($P < 0.001$) greater than that from normal erythrocytes. Iron mobilization by RSFm2phe from trophozoites was significantly ($P < 0.005$) different from that from rings. Data are given as average values ± SEs.

[b] NRBC, normal erythrocytes.

In the work described here we sought to further improve the antimalarial performance of RSFs, first, by widening the range of drug lipophilicity and, second, by designing lipophilic RSFs which can potentially generate in the cell RSFs of impermeant character. We have done that on the basis of quantitative SAR schemes and on the basis of studies of RSFs' modes of action, which relied on the chelator's ability to penetrate into the cells and extract iron, thus inducing a rapid intracellular iron deficit (28). This mode of action prevails in *P. falciparum*-infected cells because of the stage-specific and metabolically restricted capacity of the parasite to mobilize iron, primarily from the degradation of host proteins (16, 26). Chelators also affect mammalian cells, although most of them, in particular, the hydroxamate-based ones, act cytostatically, that is, only as long as they are present in the medium (5). This is because mammalian cells apparently have the capacity to replenish the cell iron stores upon removal of the chelator (5) by receptor-mediated endocytosis of transferrin. This differential action constitutes the basis for the selective cytotoxicity of the hydroxamate-based iron chelators (4, 5).

We have broadened the range of SARs by incorporating RSFs of more lipophilic (e.g., RSFm2phe and RSFm2pee) and more hydrophilic [e.g., RSFm2(H) and RSFm2pa] character (Fig. 1; Table 1). The chemical substitutions had a relatively small effect on the RSFs' rates and affinities of iron binding (Table 1). However, the antimalarial performance conformed to the lipophilic character of the new RSFs, as evident from the drug SAR studies on parasite growth (Fig. 2 and 3) and their ability to extract iron from infected cells (Table 2). Moreover, the use of potentially cleavable agents such as RSFm2pee might be advantageous on the basis of their potential to generate intracellularly impermeant chelators and lead to more persistent antimalarial effects.

Although the SAR studies indicate that RSFs' antimalarial efficacies are apparently limited by their ability to access critical iron pools or components, it is not clear whether membrane permeation per se is the sole determinant of that efficacy. The PC has conventionally been identified with the ability of molecules to permeate membranes (19). Consistent with this notion are our data on high-affinity iron-binding RSFs in erythrocyte membranes (Table 1) and other classes of iron chelators studied in both erythrocyte ghosts and living cells (32, 35). However, chelators with high PCs and similar iron-binding affinities which reach transmembrane equilibrium on a comparable time scale markedly differ in their iron extraction capacities and antimalarial efficacies. This observation implicates

PC, but not merely membrane permeation, as being important for antimalarial efficiency. Indeed, the lipophilic character might confer upon RSFs not only topographical specificity, that is, accessibility to membrane-enclosed compartments, but also chemical specificity, that is, access to particular chemical components or iron pools. The results of the studies presented in Table 2 and Fig. 6 and 7 indicate that RSFm2phe, the most lipophilic RSF used, not only was the most potent antimalarial agent but also was the most efficient RSF in extracting iron from infected cells. At present it remains to be established whether the extra iron extracted by the most lipophilic RSF is derived from a specific chemical component or a dispersed pool of the metal which is critical for parasite survival. Irrespective of the source of this extracted iron, the results offer new possibilities for further improvements in the antimalarial performance of iron chelators.

ACKNOWLEDGMENTS

This work was supported in part by NIH grant AI20342 and the Israel Science Fund administered by the Israel Academy of Science and Humanities.

We thank Rachel Lazar (Weizman Institute, Rehovot, Israel) for assistance in the synthesis of the various RSFs, Prem Ponka (McGill University, Montreal, Quebec, Canada) for the gift of SIH, and I. N. Slotki and W. Breuer (Hebrew University, Jerusalem, Israel) for critical reading of the manuscript.

REFERENCES

1. **Atamna, H., and H. Ginsburg.** 1995. Heme degradation in the presence of glutathione. A proposed mechanism to account for the high levels of non-heme iron found in the membranes of hemoglobinopathic red blood cells. J. Biol. Chem. **270:**24876–24883.
2. **Breuer, W., S. Epsztejn, P. Millgram, and Z. I. Cabantchik.** 1995. Transport of iron and other transition metals into cells as revealed by fluorescent probe. Am. J. Physiol. **268:**C1354–C1361.
3. **Bunnag, D., A. A. Poltera, A. Viravan, S. Looareesuwan, K. T. Harinasuta, and C. Schindlery.** 1992. Plasmocidal effect of desferrioxamine B in human *vivax* or *falciparum* malaria from thailand. Acta Trop. **52:**59–67.
4. **Cabantchik, Z. I.** 1995. Iron chelators as antimalarials: the biochemical basis of selective cytotoxicity. Parasitol. Today **11:**74–78.
5. **Cabantchik, Z. I., H. Glickstein, J. Golenser, M. Loyevsky, and A. Tsafack.** 1996. Iron chelators. Mode of action as antimalarials. Acta Haematol. **95:** 70–77.
6. **Cabantchik, Z. I., H. Glickstein, P. Milgram, and W. Breuer.** 1996. A fluorescence assay for assessing chelation of intracellular iron in a membrane model system and in mammalian cells. Anal. Biochem. **233:**221–227.
7. **Ceriotti, F., and G. Ceriotti.** 1980. Improved direct specific determination of serum iron and total iron-binding capacity. Clin. Chem. **26:**327–331.
8. **Dayan, I., J. Libman, Y. Agi, and A. Shanzer.** 1993. Chiral siderophore analogs: ferrichrome. Inorg. Chem. **32:**1467–1475.
9. **Dayan, I., J. Libman, A. Shanzer, C. E. Felder, and S. Lifson.** 1991. Regulation of molecular conformation of chiral, tripodal structures by Ca^{2+} binding. J. Am. Chem. Soc. **113:**3431–3439.
10. **Desjardins, R. E., C. J. Canfield, J. D. Haynes, and J. D. Chulay.** 1979. Quantitative assessment of antimalarial activity in vitro by semiautomated microdilution technique. Antimicrob. Agents Chemother. **16:**710–718.
11. **Fritsch, G., J. Treumer, D. T. Spira, and A. Jung.** 1985. Plasmodium vinckei: suppression of mouse infections with desferrioxamine B. Exp. Parasitol. **60:**171–174.
12. **Gabay, T., and H. Ginsburg.** 1993. Hemoglobin denaturation and iron release in acidified red blood cell lysate: a possible source of iron for intraerythrocytic malaria parasites. Exp. Parasitol. **77:**261–272.
13. **Golenser, J., A. Tsafack, Y. Amichai, J. Libman, A. Shanzer, and Z. I. Cabantchik.** 1995. Antimalarial action of hydroxamate-based iron chelators and potentiation of desferrioxamine action by reversed siderophores. Antimicrob. Agents Chemother. **39:**61–65.
14. **Gordeuk, V. R., G. M. Brittenham, and P. E. Thuma.** 1994. Iron chelation as a chemotherapeutic strategy in the treatment of malaria, p. 111–130. *In* R. J. Bergeron and G. M. Brittenham (ed.), The development of iron chelators for clinical use. CRC Press, Inc., Boca Raton, Fla.
15. **Heppner, D. G., P. E. Hallaway, G. J. Kontoghiorghes, and J. W. Eaton.** 1988. Antimalarial properties of orally active iron chelators. Blood **72:**358–361.
16. **Hershko, C., and T. E. A. Peto.** 1988. Deferoxamine inhibition of malaria is independent of host iron status. J. Exp. Med. **168:**375–387.
17. **Loyevsky, M., S. D. Lytton, B. Mester, J. Libman, A. Shanzer, and Z. I. Cabantchik.** 1993. The antimalarial action of desferal involves a direct access route to erythrocytic (*Plasmodium falciparum*) parasites. J. Clin. Invest. **91:**218–224.
18. **Lytton, S. D., M. Loyevsky, B. Mester, J. Libman, I. Landau, A. Shanzer, and Z. I. Cabantchik.** 1993. In vivo antimalarial action of a lipophilic iron (III) chelator: suppression of *Plasmodium vinckei* infection by reversed siderophore. Am. J. Hematol. **43:**217–220.
19. **Lytton, S. D., B. Mester, I. Dayan, H. Glickstein, J. Libman, A. Shanzer, and Z. I. Cabantchik.** 1993. Mode of action of iron (III) chelators as antimalarials. I. Membrane permeation properties and cytotoxic activity. Blood **81:** 214–221.
20. **Lytton, S. D., B. Mester, J. Libman, A. Shanzer, and Z. I. Cabantchik.** 1994. Mode of action of iron (III) chelators as antimalarials. II. Evidence for differential effects on parasite iron-dependent nucleic acid synthesis. Blood **84:**910–915.
21. **Poch, G.** 1993. Combined effects of drugs and toxic agents. Modern evaluation in theory and practice. Springer-Verlag, New York.
22. **Pollack, S., R. N. Rossan, D. E. Davidson, and A. Escjadillo.** 1987. Desferrioxamine suppresses *Plasmodium falciparum* in aotus monkeys. Proc. Soc. Exp. Biol. Med. **184:**162–167.
23. **Raventos-Suarez, C., S. Pollack, and R. L. Nagel.** 1980. Plasmodium falciparum: inhibition of *in vitro* growth by desferrioxamine. Am. J. Trop. Med. Hyg. **31:**919–922.
24. **Rivadeneira, E. M., M. Wasserman, and C. Espinal.** 1983. Separation and concentration of schizonts of *Plasmodium falciparum* by Percoll gradients. J. Protozool. **30:**367–370.
25. **Scheibel, L. W., and S. Rodriguez.** 1989. Antimalarial activity of selected aromatic chelators. V. Localization of ^{59}Fe in *Plasmodium falciparum* in the presence of oxines, p. 119–149. *In* G. Brewer (ed.), Malaria and the red cell. Alan R. Liss, Inc., New York.
26. **Scott, M. D., A. Ranz, F. A. Kuypers, B. H. Lubin, and S. R. Meshnick.** 1990. Parasite uptake of desferroxamine: a prerequisite for antimalarial activity. Br. J. Haematol. **75:**598–602.
27. **Shanzer, A., and J. Libman.** 1991. Biomimetic siderophores, p. 309–338. *In* G. Winkelmann (ed.), CRC Handbook of Microbial Iron Chelates. CRC Press, Inc., Boca Raton, Fla.
28. **Shanzer, A., J. Libman, S. D. Lytton, H. Glickstein, and Z. I. Cabantchik.** 1989. Reversed siderophores act as antimalarial agents. Proc. Natl. Acad. Sci. USA **88:**6585–6589.
29. **Trager, W., and J. B. Jensen.** 1976. Continuous culture of human malaria parasites. Science **193:**673–675.
30. **Traore, O., P. Carnevalle, L. Kaptue-Noche, J. M'Nbede, M. Desfontaine, J. Elion, D. Labie, and R. Nagel.** 1991. Preliminary report on the use of desferrioxamine in the treatment of *Plasmodium falciparum* malaria. Am. J. Hematol. **37:**206–208.
31. **Tsafack, A., J. Golenser, J. Libman, A. Shanzer, and Z. I. Cabantchik.** 1995. Mode of action of iron(III) chelators as antimalarials. III. Overadditive effects in the combined action of hydroxamate-based agents on *in vitro* growth of *Plasmodium falciparum*. Mol. Pharmacol. **47:**403–409.
32. **Tsafack, A., M. Loyevsky, P. Ponka, and Z. I. Cabantchik.** 1996. Mode of action of iron(III) chelators as antimalarials. IV. Potentiation of desferal action by benzoyl and isonicotinoyl hydrazone derivatives. J. Lab. Clin. Med. **127:**574–582.
33. **Wyler, D. J.** 1992. Bark, weeds, and iron chelators—drugs for malaria. N. Engl. J. Med. **327:**1519–1521.
34. **Yakirevitch, P., N. Rochel, A. M. Albrecht-Gary, J. Libman, and A. Shanzer.** 1991. Chiral siderophore analogs: ferrioxamines and their iron(III) coordination properties. Inorg. Chem. **32:**3431–3439.
35. **Zanninelli, G., H. Glickstein, W. Breuer, P. Milgram, P. Brissot, R. C. Hider, A. M. Konijn, J. Libman, A. Shanzer, and Z. I. Cabantchik.** Submitted for publication.